Journal of Drug Delivery Science and Technology 98 (2024) 105911

Contents lists available at ScienceDirect

Journal of Drug Delivery Science and Technology

journal homepage: www.elsevier.com/locate/jddst

Targeted polymer lipid hybrid nanoparticles for *in-vitro* siRNA therapy in triple-negative breast cancer

Meenu Mehta [a], Thuy Anh Bui [a], Andrew Care [b], Wei Deng [a,*]

[a] School of Biomedical Engineering, University of Technology Sydney, Ultimo, NSW, 2007, Australia
[b] School of Life Sciences, University of Technology Sydney, Ultimo, New South Wales, 2007, Australia

ARTICLE INFO

Keywords:
Triple-negative breast cancer
siRNA therapy
Targeted nanoparticles
Hypoxia

ABSTRACT

Triple-negative breast cancer (TNBC) is an aggressive subtype of breast cancer, characterised by a lack of hormone receptors and HER2 expression, resulting in limited treatment options and poor patient outcomes. This study explores a novel therapeutic approach using PLGA lipid nanoparticles loaded with siXBP1 and conjugated with an epidermal growth factor receptor (EGFR) antibody. This nanncarrier will silence the XBP1 gene, which is crucial for the progression and survival of TNBC, particularly in hypoxic conditions. The conjugation of nanoparticles with the EGFR antibody improves their targeting ability to TNBC cells, as confirmed by confocal microscopy and flow cytometry. The fluorescence intensity of the targeted nanoparticles was 1.45 times higher than that of the non-targeted counterparts. These nanoparticles efficiently delivered siRNA to TNBC cells, resulting in substantial XBP1 gene silencing efficacy of 75 %. Under hypoxic conditions, this gene silencing effect significantly promoted apoptosis by nearly threefold compared to normoxic conditions. These findings provide valuable insights into targeted therapies for TNBC and pave the way for further *in vivo* investigations to advance this approach toward clinical applications.

1. Introduction

Among all breast cancer subtypes, triple-negative breast cancer (TNBC) stands out as the most aggressive, comprising approximately 15 % of cases. It is characterized by the absence of human epidermal growth factor receptors 2 (HER2), progesterone receptors, and estrogen receptors [1]. TNBC is associated with a high recurrence rate and limited survival, with a 40 % mortality rate within five years of diagnosis [1][]. After metastasis, the average survival time is just 12.2 months, and the postoperative recurrence rate is approximately 25 % [2]. Chemo-radiotherapy stands as the standard of care for TNBC, yet its constraints involve drug toxicity, resistance, and late morbidity linked to high-dose radiation [3]. Due to the lack of targeted therapies specific to TNBC, there is a pressing need for innovative approaches to enhance patient outcomes [4–6].

To address this challenge, XBP1 emerges as a key driver of TNBC tumor growth and recurrence, primarily by regulating the ER stress response and unfolded protein pathways, impacting cell survival, proliferation, and chemoresistance [7,8]. Elevated XBP1 expression is frequently associated with TNBC, promoting these detrimental effects and contributing to a poor prognosis and treatment resistance [9]. Notably, a connection between XBP1 and reduced TNBC responsiveness to standard treatments is well-established [9]. Analysis of 193 TNBC patient samples revealed shorter relapse-free survival in cases with an elevated XBP1 signature [10].

Hypoxia-inducing factor 1α (HIF-1α) is known to be hyperactivated in the hypoxic microenvironment of human tumors including TNBC [11]. XBP1 has been identified to regulate tumorigenicity by controlling the HIF-1α pathway [10,12]. It can boost the stability and activity of HIF-1α, resulting in the activation of genes that support angiogenesis, glycolysis and cell survival [10,13]. XBP1 knockdown may offer a promising therapeutic approach in TNBC, particularly in hypoxic conditions. However the challenge remains in achieving precise and efficient gene silencing within TNBC cells due to limited drug delivery options.

Given significant roles of XBP1 in driving TNBC tumor growth and recurrence, specific XBP1 inhibition in TNBC tumor is a potential therapeutic approach which relies on two key challenges: basis of genetic approach and efficiency delivery vehicles specific to target cells. In the context of XBP1 gene knockdown, small interfering RNA (siRNA) offers a promising strategy for targeted gene silencing in TNBC treatment. By leveraging the RNA interference (RNAi) pathway, siRNA can selectively

* Corresponding author.
E-mail address: wei.deng@uts.edu.au (W. Deng).

https://doi.org/10.1016/j.jddst.2024.105911
Received 4 March 2024; Received in revised form 27 May 2024; Accepted 22 June 2024
Available online 22 June 2024

downregulate crucial genes, inhibiting tumor growth and overcoming treatment resistance [14]. Regarding delivery vehicles, nanoparticle-based drug delivery systems, including lipid nanoparticles with polymers like Poly (lactic-co-glycolic acid) (PLGA), are advantageous for cancer therapy [15,16]. They are noted for their biocompatibility, controlled drug release, and capacity to encapsulate diverse therapeutic agents, such as siRNA [17,18]. Within PLGA lipid nanoparticle, the lipid component ensures stability, biocompatibility, and enhanced cellular uptake via intracellular delivery of therapeutic contents, while the PLGA polymer enables controlled release and safeguards the encapsulated siRNA cargo [19].

The goal of this study was to devise a targeted therapeutic strategy for triple-negative breast cancer (TNBC) by engineering epidermal growth factor receptor (EGFR) antibody conjugated siXBP1 loaded PLGA lipid nanoparticles. We selected the EGFR antibody due to its elevated expression in TNBC, aiming to enhance siRNA delivery specificity [20].

To achieve this goal, we first characterized the synthesized nanoparticles for their particle size, zeta potential, and surface morphology, ensuring suitability for TNBC targeted delivery. Next, we examined the cellular uptake of the EGFR antibody-conjugated PLGA lipid nanoparticles in TNBC cells (MDA-MB-231) using confocal microscopy and flow cytometry as assessment of nanoparticle internalization. We confirmed EGFP gene silencing in HEK293-EGFP cells by encapsulating EGFP siRNA for confocal microscopy analysis prior to validation of XBP1 gene silencing in MDA-MB-231 cells with siXBP1-loaded PLGA lipid nanoparticles by qRT-PCR and Western Blot. Finally, we evaluated the effect of XBP1 gene knockdown with EGFR antibody-siXBP1-loaded PLGA lipid nanoparticles on cell survival and apoptosis in MDA-MB-231 cells under hypoxic conditions, highlighting the potential of our nanoparticles as a promising therapeutic approach for TNBC.

2. Materials and methods

2.1. Materials

Poly(D,L-lactide-co-glycolide) acid terminated, lactide:glycolide 50:50 (PLGA) (719,870-5G), Mw 24,000–38000, Poly vinyl alcohol (PVA) (P8136), MW 30,000–70,000, Coumarin-6 (C-6) (442,631-1G) were purchased from Sigma-Aldrich Pty Ltd (Australia). DOTAP (890890 P-200 mg) and 1,2-distearoyl-*sn*-glycero-3-phosphoethanolamine-N-[maleimide(polyethylene glycol)-2000] (ammonium salt) (DSPE-PEG2000-Mal) (880126p-25mg) were purchased from Avanti Polar Lipids. Chloroform (C2432–500 mL), Dichloromethane (270,997-1 L), Phosphate buffered saline (P4417-50 TAB) were also purchased from Sigma-Aldrich Pty Ltd (Sydney, Australia). Human anti-EGFR antibody (cetuximab, C225) was purchased from Assay Matrix Pty Ltd (Melbourne, Australia). Scramble siRNA (siScr -SIC001) was purchased from Merck, Australia and siRNA targeting EGFP (siGFP-51-01-05-06) was purchased from Integrated DNA Technologies, Australia. siRNA targeting XBP1 (s14913), Lipofectamine RNAiMax transfection reagent (13,778,075), Opti-Minimal Essential Medium (Opti-MEM; reduced serum medium; product, 31,985,062), Pierce™ Coomassie (Bradford Protein Assay Kit) (23,200) were purchased from (Thermo Fisher Scientific, Australia). MTT (3-[4,5-dimethylthiazol-2-yl]-2,5-diphenyl tetrazolium bromide), Dimethyl sulfoxide (DMSO), DAPI were purchased from Sigma-Aldrich, St. Louis, MO, USA. FITC Annexin V Apoptosis Detection Kit I (cat. no. 556547) was purchased from BD Biosciences (San Jose, CA, USA). The antibodies to XBP1 and β-actin were purchased from Abcam. All the remaining chemical reagents and solvents were purchased from Sigma-Aldrich unless stated.

2.2. Cell culture

MDA-MB-231 and MCF-7 cell lines were a kind gift from Prof. Majid Ebrahimi Warkiani lab, School of Biomedical Engineering, University of Technology Sydney, Australia. These cells were cultured in Dulbecco's Modified Eagle's Medium (DMEM) (Sigma-Aldrich Pty Ltd, Australia) with 10 % heat-inactivated Fetal Bovine Serum (Thermo Fisher Scientific, Australia) at 37 °C at 5 % CO_2 in a humidified atmosphere. Human mammary epithelial cells (HMEC) and Human embryonic kidney 293 cells expressing EGFP (HEK 293-EGFP) were a kind gift from Prof. Ewa Goldys lab, School of Biomedical Engineering, University of New South Wales, Australia. HMEC were cultured in HMEC growth medium while HEK 293-EGFP cells were cultured in DMEM with10 % heat-inactivated Fetal Bovine Serum under standard conditions (37 °C, 5 % CO_2) in a humidified incubator. All cells were frequently tested for the presence of mycoplasma, and all experiments were carried out in mycoplasma negative cells.

Table 1
Composition of different PLGA lipid nanoparticles.

S. No.	Formulation	Cargo amount	PLGA/ DOTAP ratio (w/w)	PVA (% w/ v)	DSPE-PEG2000-Mal (mg)
1.	Blank PLGA lipid nanoparticles	–	7:3	1	0.3
2.	Coumarin-6 loaded nanoparticles (C-6 NPs)	17.5 μg	7:3	1	0.3
3.	EGFP siRNA loaded nanoparticles (siEGFP NPs)	100 pmole	7:3	1	0.3
4.	Scramble siRNA loaded nanoparticles (Scr NPs)	200 pmole	7:3	1	0.3
5.	siXBP1 (siRNA) loaded nanoparticles	200 pmole	7:3	1	0.3

2.3. Methods

2.3.1. Preparation of PLGA lipid nanoparticles

PLGA lipid nanoparticles were prepared using the double emulsion-solvent evaporation technique [18]. The formulation was optimized including the particle size, zeta potential and polydispersity index (PDI) based on DOTAP/PLGA ratio, sonication time and polyvinyl alcohol (PVA) concentration. In brief, 200 pmole of siRNA was added dropwise to 500 μl of PLGA/DOTAP mixture (mole ratio of 7:3) in dichloromethane (DCM). This mixture was emulsified using probe sonication over an ice bath at 40 % amp for 30 s (3 times) to form the primary emulsion. Subsequently, 6 ml of 1 % (w/v) PVA containing 0.3 mg of DSPE-PEG2000-Mal was added to the primary emulsion, followed by sonication at 40 % amp for 30 s (3 times) over an ice bath. This process resulted in the formation of the secondary water-in-oil-in-water emulsion, which was left under agitation for 3 h at room temperature to evaporate organic solvent. Afterwards, the dispersion was centrifuged for 12 min at 4 °C and 18,000×*g*. The supernatant was discarded, and the pellet containing the nanoparticles was re-dispersed in phosphate buffer saline (PBS). This process of centrifugation and re-dispersion was repeated three times to ensure the removal of PVA before further characterisation. We employed the same method to prepare various types of PLGA lipid nanoparticles, by encapsulating different cargoes (coumarin-6 (a dye), EGFP siRNA, scramble siRNA). The formulation details are listed in Table 1.

2.3.1.1. Antibody conjugation to nanoparticles. Antibody conjugation to nanoparticles was achieved through a thiol-maleimide reaction [21]. Initially, 10 μl EGFR antibody (1 mg/ml stock solution in PBS) was diluted with 990 μl of PBS (pH 7.4). Simultaneously, 1 mg of N-Succinimidyl S-Acetylthioacetate (SATA) was dissolved in 0.5 ml of dimethyl sulphoxide (DMSO) just before the reaction. The EGFR antibody solution was then mixed with SATA solution at a molar ratio of 8:1 (SATA: antibody) and incubated at room temperature for 30 min. To facillitate

SATA crosslinking with maleimide groups, the sulfhydryl groups were deacetylated by mixing the SATA/antibody solution with 100 μl of hydroxylamine solution (0.5 M Hydroxylamine, 25 mM EDTA in PBS, pH 7.2–7.5) and incubated for 1 h at room temperature. Subsequently, conjugation was initiated by combining nanoparticles with the SATA/antibody solution at a molar ratio of 1:10 (nanoparticles: SATA/antibody solution) and incubated at room temperature for 2 h, followed by overnight incubation at 4 °C. Unbound antibody was removed through centrifugation, and the nanoparticle pellet was redispersed in PBS for further applications.

2.3.1.2. Quantification of EGFR antibody conjugated onto the surface of nanoparticles. The amount of EGFR antibody conjugated to the nanoparticle surface was confirmed by Bradford assay, which was based on the binding of coomassie brilliant blue dye (Bradford reagent) to proteins, resulting in a color change proportional to the protein concentration. Following the manufacturer's protocol, various concentrations of the protein standard solution, ranging from 25 μg/mL to 2000 μg/mL, were prepared in PBS buffer. Next, 5 μL of each standard or nanoparticle suspension was carefully transferred to the appropriate wells of a microplate. Subsequently, 250 μL of the Bradford reagent was added to each well, and the plate was incubated for 10 min at room temperature. The absorbance was measured at 595 nm using a Tecan plate reader. The amount of conjugated antibody was determined by assessing the absorbance intensity and subsequently calculating its concentration using the standard curve of free protein solution.

2.3.2. Nanoparticle characterization

Particle size, polydispersity index (PDI), and zeta potential measurements were carried out using Dynamic Light Scattering (Malvern Zetasizer Nano ZS). Before analysis, the nanoparticle suspension was resuspended, sonicated, and vortexed. For particle size and PDI measurement, diluted samples were placed in clear disposable cuvettes, while zeta cells were utilized for zeta potential measurement. All measurements were performed in triplicate at 25 °C. The surface morphology of nanoparticles was examined by using Scanning Electron Microscopy (SEM, Zeiss Supra 55 VP). For SEM imaging, nanoparticles were suspended in nuclease-free water (100 μl/ml) and sonicated for 30 s. A drop of this suspension was deposited on a silicon wafer and allowed to air dry for 24 h under ambient conditions. The silicon wafer was then attached to a stub using double-sided carbon tape. To ensure conductivity, the nanoparticles were sputtered with gold/palladium using the Leica Coater prior to image acquisition.

2.3.3. Entrapment efficiency (EE)

The amount of coumarin-6 (C-6) encapsulated within the nanoparticles was determined by assessing the fluorescence intensity of the C-6-loaded nanoparticles (C-6 NPs) (Ex/Em: 450 nm/505 nm) and subsequently calculating its concentration using the standard curve derived from a free C-6 solution.

The entrapment efficiency of siRNA loaded inside the nanoparticles was determined using RediPlate 96 Ribogreen RNA Kit (Thermo Fisher Scientific, Australia). The RiboGreen® reagent specifically reacts with free siRNA, producing a fluorescent compound with an emission maximum at 535 nm (λex = 485 nm). Thus, to assess entrapment efficiency, the prepared nanoparticle suspension was centrifuged and the supernatant was collected. The unloaded siRNA in the supernatant was then measured using the Ribogreen RNA Kit and compared to the initial siRNA concentration used in the nanoparticle preparation.

In details, various concentrations of pure siRNA solution (ranging from 5 ng/mL to 200 ng/mL) were prepared using TE buffer. Subsequently, 20 μL pure siRNA solution and the supernatant were added to wells of a microplate, followed by thorough pipetting. The microplate was incubated for 20 min at room temperature, shielded from light. After incubation, fluorescence was measured using a microplate reader (Ex/Em: 480 nm/535 nm). The concentration of siRNA in the supernatant was determined by comparing it to the standard curve of a free siRNA solution. The entrapment efficiency was calculated using the following equation:

$$\%EE = \frac{(\text{RNA amount used for formulation} - \text{RNA amount present in supernatant})}{\text{RNA amount used for formulation}} x100$$

Table 2
Primer sequences used for qRT-PCR.

Primer	Sequence
XBP1 - Forward	5′- AGGAGTTAAGACAGCGCTTGGGGATGGAT-3′
XBP1 - Reverse	5′-CTGAATCTGAAGAGTCAATACCGCCAGAAT-3′
Beta actin – Forward	5′-CCTGTACGCCAACACAGTGC-3′
Beta actin – Reverse	5′-ATACTCCTGCTT GCTGATCC-3′

2.3.4. Cellular uptake activity

Cellular uptake activity was assessed by using C-6 NPs and EGFR antibody conjugated C-6 nanoparticles (EGFR Ab-C-6 NPs). Briefly, 5×10^4 MDA-MB-231 cells were cultured overnight in glass-bottom petri dishes and incubated with nanoparticle suspension (200 μg/ml) for 1 and 2 h, respectively. Subsequently, the cells were thoroughly washed with DPBS (pH 7.4) three times to eliminate any unbound nanoparticles and then fixed using 4 % paraformaldehyde (100 μl) at room temperature. After fixation, the cells were stained with DAPI (Sigma) reagent, and the internalization of nanoparticles was visualized using a Nikon A1 inverted confocal microscope system. Additionally, flow cytometry analysis was performed after the nanoparticle incubation. The cells were washed, trypsinized, collected, and their fluorescence was quantitatively analyzed using a CytoFLEX LX flow cytometer (Beckman Coulter).

2.3.5. XBP1 expression level in normal vs breast cancer cell lines and under hypoxia conditions

To evaluate XBP1 gene expression, we selected two breast cancer cell lines, MDA-MB-231 and MCF-7, along with one normal mammary epithelial cell line (HMEC). To induce hypoxia, MDA-MB-231 cells were placed in hypoxic chamber for 24 h or 48 h. After each incubation period, RNA and proteins were isolated from cells and analyzed for XBP1 gene expression.

2.3.5.1. RNA extraction. RNA samples were isolated using the Trizol® method [22]. Initially, the cells underwent a brief wash in PBS, followed by transfer into nuclease-free Eppendorf tubes. Subsequently, they were centrifuged at 12,000×*g* at 4 °C for 10 min. The resulting cell pellets were then combined with 1 ml of Trizol® (Invitrogen), and 300 μl was added, after which the mixture was incubated at room temperature for 3 min. After this, the samples were subjected to phase separation by centrifuging at 12,000×*g* at 4 °C for 10 min. The upper aqueous layer, containing the RNA, was carefully transferred to new tubes containing 600 μl of ice-cold isopropanol (Sigma, Australia). RNA precipitation was facilitated by centrifuging for 30 min at 12,000×*g* and 4 °C. The RNA pellets were briefly washed in 1 ml of 70 % ethanol and again centrifuged at 12,000×*g* at 4 °C for 10 min. Following this step, the ethanol

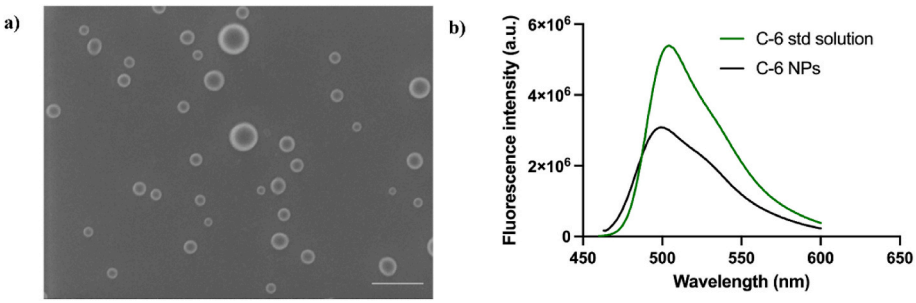

Fig. 1. a) The SEM image of blank PLGA lipid nanoparticles (Scale bar = 200 nm); b) Fluorescence emission spectra of coumarin-6 solution (C-6 std solution) and coumarin-6 loaded nanoparticles (C-6 NPs).

was removed, and the RNA pellet was dried on a 37 °C heat block for 5 min. Finally, the resulting RNA pellet was resuspended in 40 μl of nuclease-free water. RNA concentration was measured via absorbance at 260 nm by Nanodrop™ One Microvolume UV–Vis spectrophometer (Thermo Fisher Scientific, Australia).

2.3.5.2. qRT-PCR. All the primers utilized in the quantitative PCR reactions for this study were purchased from Sigma-Aldrich. In summary, a quantity of RNA samples less than 1 μg was employed for both cDNA conversion and the qPCR reaction, employing the Luna® Universal One-Step RT-qPCR Kit from New England Biolabs. The qPCR reactions were conducted according to the manufacturer's protocol. The primer sequences used for these reactions are detailed in Table 2.

2.3.5.3. Protein extraction. Cell samples were gathered in RIPA Lysis buffer, which included Halt™ Protease Inhibitor Cocktail (Thermo Fisher Scientific, Australia). They were left to incubate on ice for 20 min before undergoing a short 15-s sonication. Subsequently, the cell lysates were subjected to centrifugation at 12,000×*g* at 4 °C for 20 min to eliminate cellular debris. The protein concentration of each sample was assessed via absorbance at 280 nm using the NanoDrop™ Microvolume UV–Vis Spectrophotometer (Thermo Fisher Scientific, Australia).

2.3.5.4. Western blot assay. Briefly, 30 μg of each protein lysate was combined with 5 μl of NuPAGE LDS Sample Buffer and heated at 70 °C for 10 min. All prepared samples were subsequently loaded into NuPAGE 4–12 % Bis-Tris 1.5 mm Mini Protein Gels secured within the XCell SureLock™ Mini-Cell. The loaded protein samples were then separated in 1 × NuPAGE MOPS SDS Running Buffer at 125 V for 90 min.

After the gel electrophoresis, the protein samples were transferred onto a 0.2 μm PVDF Transfer Membrane using the XCell Blot Module and 1 × NuPAGE Transfer Buffer at 30 V for 120 min. The membranes were subsequently immersed in a blocking solution (3 % w/v Bovine Serum Albumin from Sigma in TTBS buffer, which consists of 0.01 M Tris Base, 0.05 M NaCl, and 0.1 % Tween20) for 1 h at room temperature to prevent non-specific binding.

Membrane incubation with primary antibodies (XBP1 or Beta-actin from Abcam, each at a 1:1000 dilution in TTBS) was carried out at 4 °C overnight. After three 5-min washes in TTBS buffer, the membranes were incubated in an anti-rabbit horse peroxidase-conjugated secondary antibody (CST, diluted at 1:5000 in TTBS) on an orbital shaker at room temperature. Following this, the membranes were washed in TTBS buffer for 5 min each and then visualized using PierceTM ECL Western Blotting Substrate (Thermo Fisher Scientific, Australia) under a Chem-iDoc MP System (Biorad, USA).

2.3.6. Assessment on in vitro EGFP and XBP1 knockdown via siRNA-loaded nanoparticles

HEK293-EGFP cells were cultured at a density of 5 × 10^4 in glass-bottom petri dishes and then incubated with the siGFP-loaded nanoparticle suspension (10 nM) for 24 and 48 h. Subsequently, the cells were imaged under a confocal microscope to assess EGFP fluorescence signal. Additionally, flow cytometry analysis was performed as indicated in the above section.

MDA-MB-231 cells were seeded at a density of 1 × 10^5 cells per well in a 6-well plate and incubated for 24 h. Following this, the cells were treated with various conditions for an additional 48 h. The treatment conditions included: cells only, free siRNA alone, siRNA transfected with RNAiMax transfection reagent, EGFR antibody conjugated siXBP1-loaded nanoparticles (EGFR Ab-siXBP1 NPs) and EGFR antibody conjugated siScr-loaded nanoparticles (EGFR Ab-Scr NPs). All these samples contain 25 nM siXBP1 or siScr. After incubation period, cellular RNA was collected using the same method followed by RT-PCR analysis.

2.3.7. In-vitro cell viability assay

Cells were seeded at a density of 1 × 10^4 cells per well in 96-well plates with culture medium containing 10 % FBS for 24 h. After 24 h, the cells were treated with different concentrations of nanoparticles (200–400 μg/ml) for 48 h. Following this treatment period, 10 μl of Thiazolyl Blue Tetrazolium Bromide (Sigma) at a concentration of 5 mg/ml in sterile PBS was added to each well and incubated for 4 h at 37 °C in 5 % CO_2. After removing the supernatant, 100 μL of DMSO was added to dissolve the formazan crystals, resulting in the formation of a purple-colored product. The absorbance of this product was measured using a Tecan plate reader at 570 nm. The cell viability was calculated as a percentage of the absorbance in the treated cells compared with that of untreated cells, as follows:

$$\text{Viability (\%)} = (A_g - A_{blank})/(A_c - A_{blank}) \times 100$$

Where A_g is the absorbance of each group, A_c is the absorbance of the control group and A_{blank} is the absorbance of cell culture medium.

2.3.8. Cellular apoptosis assay

For apoptosis assays, 1 × 10^5 cells per well were seeded into 6-well plates in two separate sets. One set was incubated in normal incubator while the other was placed in hypoxic chamber for 48 h to induce hypoxia. After the respective incubation periods, the cells were exposed to EGFR Ab-siXBP1 NPs and EGFR Ab-siScr NPs maintained for an additional 48 h within the hypoxic chamber. The treatment groups consisted of control (cells only), cells treated with antibody-conjugated siXBP1 loaded nanoparticles, and cells treated with antibody-conjugated siScr-loaded nanoparticles. After 48 h of treatment, apoptosis was quantified using the FITC Annexin V Apoptosis Detection Kit I (cat. no. 556547; BD Biosciences) following the manufacturer's instructions. Cells were harvested and washed twice with PBS. Subsequently, 1 × 10^6 cells were resuspended in 100 μl of 1 × binding buffer (diluted with ddH_2O), followed by the addition of 5 μl FITC and 5 μl PI to each tube. The samples were incubated for 30 min at room temperature in darkness. After staining, 500 μl of 1 × binding buffer was added to each tube and analyzed by flow cytometry. Similar experiments were conducted under non-hypoxic conditions.

Table 3
Characterization of prepared PLGA lipid nanoparticles.

Samples	Particle size (nm)	PDI	Zeta Potential (mV)	Entrapment Efficiency (%)
Blank PLGA lipid nanoparticles	163 ± 2.02	0.05 ± 0.02	25.9 ± 0.25	–
Coumarin-6 loaded nanoparticles (C-6 NPs)	186.08 ± 7.1	0.06 ± 0.03	19.4 ± 0.37	73.37 ± 1.7
EGFP siRNA loaded nanoparticles (siGFP NPs)	178.9 ± 9.2	0.05 ± 0.02	14.2 ± 0.15	94.92 ± 2.9
EGFR antibody-conjugated Coumarin-6 loaded nanoparticles (EGFR Ab-C-6 NPs)	209.2 ± 1.3	0.25 ± 0.03	−2.92 ± 0.37	56.11 ± 1.4
EGFR antibody-conjugated siXBP1 loaded nanoparticles (EGFR Ab-siXBP1 NPs)	226.7 ± 8.7	0.35 ± 0.02	−3.08 ± 0.17	82.96 ± 2.4
EGFR antibody- conjugated siScr loaded nanoparticles (EGFR Ab-Scr NPs)	208.9 ± 4.5	0.14 ± 0.05	−0.791 ± 0.14	83.45 ± 2.8

3. Results

3.1. Preparation and characterization of nanoparticles

In this study, lipid polymer hybrid nanoparticles were prepared via double emulsion solvent evaporation technique. The morphology of prepared nanoparticles was evaluated under SEM. Fig. 1a revealed that the blank nanoparticles had a spherical shape with an average size 150 ± 7.4 nm. From DLS measurements, the average size of blank nanoparticles, C-6 loaded nanoparticles and EGFP siRNA loaded nanoparticles was about 163 ± 2.02 nm, 186.08 ± 7.1 nm, and 178.9 ± 9.2 nm, respectively (Table 3). These samples exhibited a positively charged surface, and their low polydispersity index (PDI) indicated that they were uniform in size and monodispersed.

To enhance the ability of the nanoparticles to target cancer cells, we attached targeting molecules, EGFR antibody to the surface of the nanoparticles. For conjugated samples, we observed a slight increase in size, changing from 186.08 ± 7.1 nm to 209.2 ± 1.3 nm. There was also a concurrent increase in PDI from 0.05 ± 0.02 to 0.35 ± 0.02 (Table 3). These changes fall within acceptable thresholds, indicating a homogeneous nanoparticle population [23]. In order to quantify the amount of EGFR antibody conjugated with the nanoparticles, a colorimetric Bradford protein assay was performed, with about 68.8 % of EGFR antibody being successfully conjugated with the nanoparticles. This finding closely aligns with other reported studies [24].

We further assessed the cargo loading efficacy of these nanoparticles. As shown in Fig. 1b, there was a typical fluorescence peak at 505 nm wavelength of the C-6 observed in C-6 loaded nanoparticles, indicating the successful loading of C-6 within the nanoparticles. For C-6 NPs, the entrapment efficiency was calculated to be 73.37 % (Table 3). For conjugated nanoparticles, the entrapment efficiency was reduced to 56.11 % (Table 3), possibly attributed to losses incurred during the secondary centrifugation step carried out after antibody conjugation. Regarding siRNA, the highest loading efficiency of 94.92 % was observed in siGFP nanoparticles. This could be attributed to the electrostatic interactions between the positively charged lipid compound and the negatively charged siRNA.

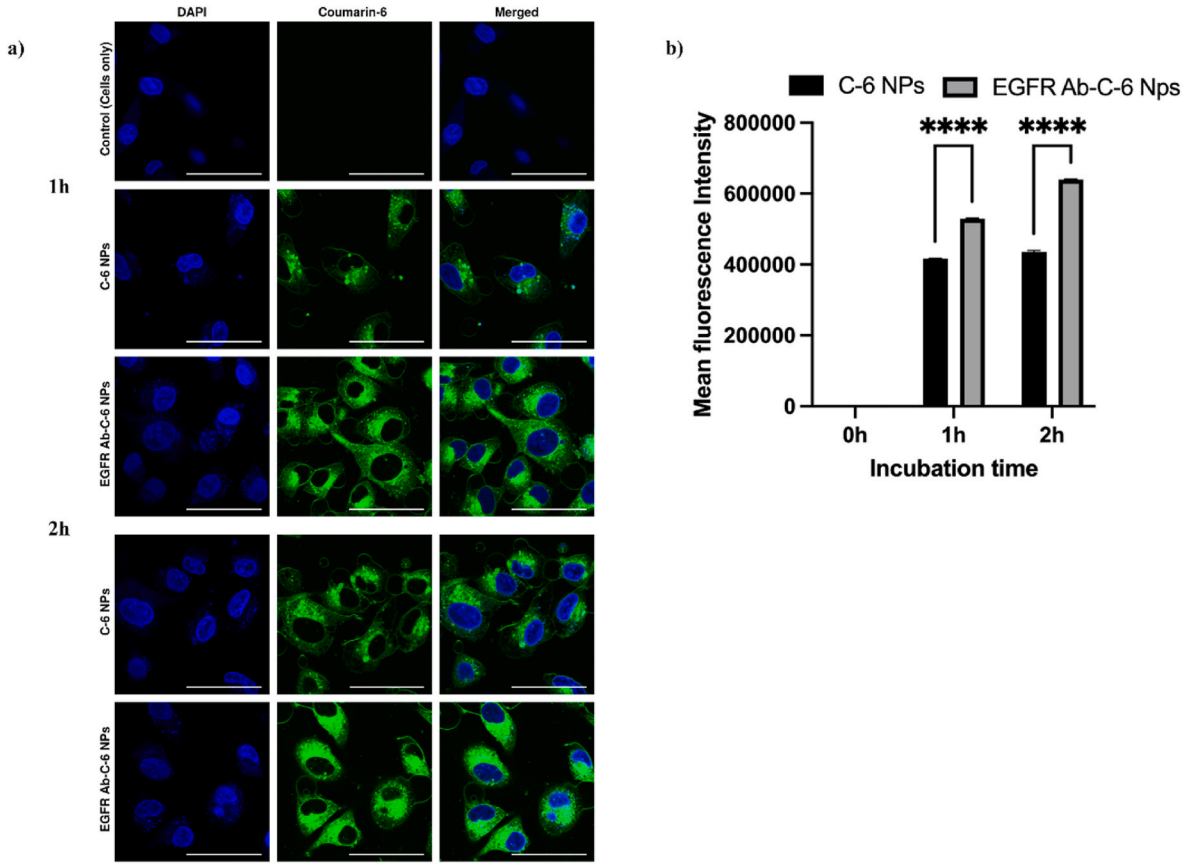

Fig. 2. a) Confocal microscopic images of MDA-MB-231 cells after incubation with C-6 NPs and EGFR AB-C-6 NPs; The scale bar is 50 μm b) The mean fluorescence intensity of C-6 in MDA-MB-231 cells treated with C-6 NPs and EGFR AB-C-6 NPs measured by flow cytometry. Data represented as mean ± s.e.m., (n = 3). ****p < 0.0001.

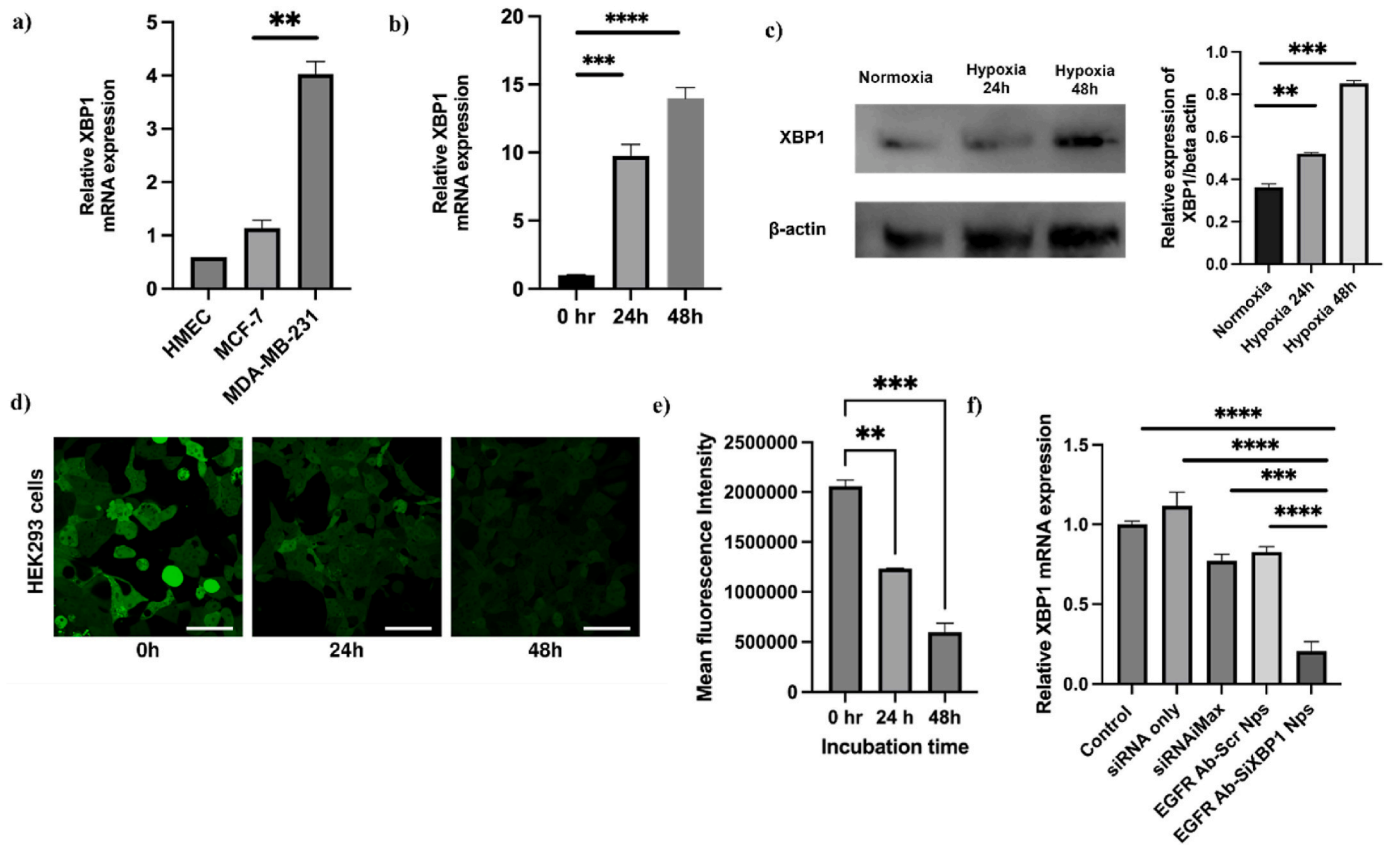

Fig. 3. a) XBP1 mRNA expression in normal and breast cancer cell lines.; b) XBP1 mRNA expression in MDA-MB-231 under hypoxic conditions; c) Western blot and densitometric analysis of XBP1 protein expression in MDA-MB-231 cells under hypoxic conditions (d) Confocal microscopic images of HEK293-EGFP cells after the treatment with 100 μg/ml of siGFP NPs, the scale bar is 50 μm; e) The mean fluorescence intensity of EGFP positive cells; f) XBP1 mRNA expression in MDA-MB-231 cells after treatment with 25 nM of naked siRNA, 200 μg/ml of EGFR Ab-siXBP1 NPs (contains 25 nM siRNA), 200 μg/ml of EGFR Ab-Scr NPs (contains 25 nM siRNA), and siXBP1 with RNAiMax (25 nM). Data represented as mean ± SEM; n = 3; **p < 0.01; ***p < 0.001; ****p < 0.001.

3.2. *In-vitro cellular uptake study*

To achieve the targeting capability of our nanoparticles on TNBC cells, we conjugated the nanoparticles with EGFR antibody. This modification specifically targets the EGFR receptor, which is known to be overexpressed in approximately 50 % of TNBC cells compared to other breast cancer subtypes [25]. This strategy was reported an effective targeting tool for TNBC cells, leading to increased cellular drug accumulation and enhanced treatment efficacy [26]. The targeting capability of antibody conjugated nanoparticles was assessed by comparing the cellular uptake of EGFR Ab-C-6 NPs and non-targeted C-6 NPs in MDA-MB-231 cells at different incubation times. Fig. 2a demonstrated the higher C-6 fluorescence signal from the cells treated by targeted nanoparticles compared with non-targeted ones. As shown in Fig. 2b, the fluorescence intensity of C-6, measured via flow cytometry, demonstrated approximately 1.26-fold and 1.45-fold higher values for EGFR Ab-C-6 NPs compared to non-targeted counterparts at 1 h and 2 h incubation times, respectively. This enhanced internalization capability of targeted nanoparticles was probably attributed to the specific affinity interaction between anti-EGFR antibody and overexpressed EGFR on the surface of cancer cells.

3.3. *Assessment on in-vitro EGFP and XBP1 knockdown via nanoparticles*

We first assessed XBP1 gene expression in two breast cancer cell lines, MDA-MB-231 and MCF-7, along with a normal breast cell line, HMEC. As illustrated in Fig. 3a, a significantly higher XBP1 mRNA expression was observed in MDA-MB-231 cells compared to MCF-7 and HMEC cell lines. Existing literature indicates that hypoxia triggers the activation of XBP1 expression, in conjunction with its co-regulator, HIF-1α, in TNBC tissues, thereby promotes cancer progression [10]. Thus, we investigated the effect of hypoxia on XBP1 expression in MDA-MB-231 cells. As shown in Fig. 3b, XBP1 mRNA expression apparently increased under hypoxic conditions, which was further supported by Western blot analysis (Fig. 3c).

Following the confirmation of XBP1 gene expression levels in MDA-MB-231, we evaluated the efficacy of gene knockdown using our nanoparticles. We first validated the transfection feasibility of our nanoparticles targeting EGFP in HEK293 cells. Fig. 3d demonstrates an apparent decrease in EGFP fluorescence intensity in the cells treated with 100 μg/ml of siGFP NPs for 24 and 48 h compared with the control. Flow cytometry data further revealed reductions of 42.83 % and 72 % in EGFP intensity at 24 h and 48 h post-transfection, respectively (Fig. 3e), indicating the nanoparticles are capable of effectively suppressing the EGFP gene expression. After confirming that our nanoparticles successfully delivered EGFP siRNA in HEK293 cells, we further assessed the transfection effectiveness of our formulation targeting XBP1 gene in MDA-MB-231. As shown in Fig. 3f, the assessment of XBP1 mRNA expression levels was conducted under various treatment conditions, including EGFR Ab-siXBP1 NPs, EGFR Ab-Scr NPs, siXBP1 with RNAiMax and naked siXBP1 only. Among these treatments, we noted that approximately 75 % reduction in XBP1 gene expression in MDA-MB-231 cells at 48 h after treatment with EGFR Ab-siXBP1 NPs. By contrast, the commercial transfection reagent (siXBP1 with RNAiMax) achieved only around 30 % suppression of XBP1gene expression.

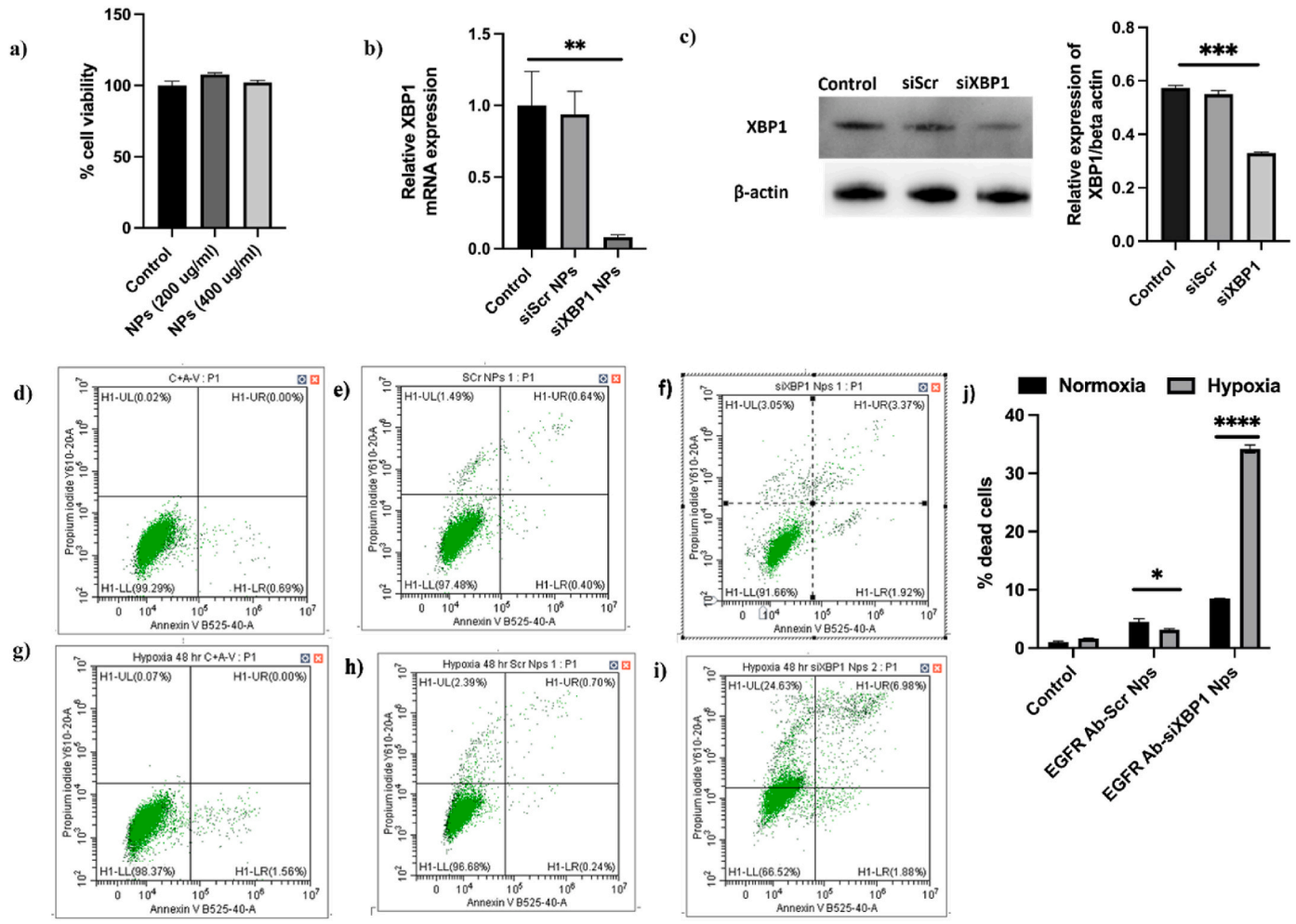

Fig. 4. a) Cell viability of MDA-MB-231 cells after treatment with different concentrations of blank PLGA lipid nanoparticles; b) XBP1 mRNA expression in MDA-MB-231 cells after treatment with 200 μg/ml of EGFR Ab-siXBP1 NPs and EGFR Ab-Scr NPs under hypoxic conditions; c) Western blot and densitometric analysis of XBP1 protein expression level after the same treatments; (d–i) FITC-Annexin V/PI flow cytometry plots of MDA-MB-231 cells after different treatments indicated in the figures; (j) Represent % of dead cells based on flow cytometry plots. Data represented as mean ± SEM; n = 3; *p < 0.1; ****p < 0.001.

3.4. Investigation of cellular apoptosis after the XBP1 gene knockdown

Before assessing the effect of XBP1 gene knockdown on cellular apoptosis, we first examined the cellular toxicity of our nanoparticles in MDA-MB-231 cells via MTT assay. As shown in Fig. 4a, no significant change in cell viability was observed when treated with blank PLGA lipid NPs at concentrations of 200 μg/ml (the concentration used for gene delivery) and even at a higher concentration of 400 μg/ml, compared with the control group. This observation indicates that our nanoparticles are unlikely to adversely impact the viability of MDA-MB-231 cells in our study.

As illustrated in Fig. 3c, hypoxia induces an upregulation in XBP1 protein expression levels. In line with this observation, we further assessed the XBP1 gene knockdown efficacy of the nanoparticles under hypoxic conditions, which are representative of the TNBC cell environment. As shown in Fig. 4b, cells treated with EGFR Ab-siXBP1 NPs demonstrated a significant reduction of approximately 90 % in XBP1 mRNA expression. Consistent with the decrease in mRNA levels, the expression level of XBP1 proteins was also reduced, as illustrated in Fig. 4c.

Furthermore, an apoptosis and necrosis assay were conducted to determine the impact of XBP1 gene silencing on the cell death pathways. As displayed in Fig. 4f and j, the cells treated with EGFR Ab-siXBP1 NPs under normal conditions exhibited low-level apoptosis and necrosis, only being 7 ± 1.9 %. This indicated that XBP1 gene knockdown showed negligible cytotoxicity to cancer cells under normal conditions. However, the higher percentage of dead cells was observed when the EGFR Ab-siXBP1 NP treatment occurred under hypoxic conditions, being 34 ± 2.4 % (Fig. 4i and j). Correspondingly, the percentage of healthy cells in this group reduced to about 66 ± 2.6 %, compared to the control group (98.37 ± 1.2 %, Fig. 4j). Collectively, these findings suggest that the percentage of dead cells following XBP1 gene knockdown increases nearly threefold when cells are exposed to a hypoxic microenvironment compared to normal conditions.

4. Discussion

TNBC, marked by the absence of ER, PR, and HER2 expression, display insensitivity to endocrine therapy and HER2-targeted treatments, which led to a major challenge in developing a safe and effective treatment for TNBC [27,28]. Recent studies have discovered the critical role of the unfolded protein response (UPR) regulator XBP1in fostering tumorigenesis and recurrence specifically in TNBC, making it a potential therapeutic target to treat TNBC [10]. The primary obstacle for targeting XBP1 in TNBC cells was mainly focused on achieving both efficient gene knockdown and specificity for TNBC cells [28]. To address this issue, this study focused on developing and investigating the effectiveness of PLGA lipid nanoparticles in knocking down XBP1 specifically in TNBC

cells.

We successfully developed and characterized the lipid-polymer nanoparticles. We optimized their size, zeta potential, and surface morphology to ensure their suitability for targeted delivery. We achieved a high entrapment efficiency of siRNA in our nanoparticles, a critical factor for effective gene silencing. Furthermore, the successful conjugation of EGFR antibodies to these nanoparticles enables their enhanced cellular uptake activity in TNBC cells, as demonstrated in Fig. 2. This enhanced cellular uptake aligns with prior research reporting the effectiveness of EGFR-conjugated nanoparticles in targeting to breast cancer cells [29]. Importantly, our findings in Fig. 4a demonstrate that these nanoparticles did not induce toxicity in MDA-MB-231 cells. This delivery system has demonstrated higher XBP1 transfection efficacy in MDA-MB-231 cells compared with commercial alternatives (Fig. 3f). These nanoparticles (25 nM) resulted in approximately 75 % XBP1 gene knockdown in MDA-MB-231 cells at 48 h post-transfection, whereas commercial transfection reagents achieved only around 30 % reduction of XBP1 gene expression. These results were consistent with other reported research, where approximately 80–85 % XBP1 gene knockdown efficacy was achieved using antibody-conjugated siXBP1-loaded nanoparticles [30,31]. We particularly focused on the gene silencing efficacy under hypoxic environment, a condition known to induce cancer cell metabolic adaptation, survival, and therapy resistance [10]. Our results revealed that our nanoparticles achieved a significant reduction in XBP1 mRNA expression of approximately 90 % even under the challenging hypoxic environment (Fig. 4b).

Apoptosis is a crucial pathway leading to the cancer cell death specifically under hypoxic condition. We found out that XBP1 silencing did not alter cell apoptosis under normal conditions (Fig. 4d–f), which aligns with previously reported studies [30,31]. However, in hypoxic conditions where XBP1 expression is upregulated (Fig. 3b), we noted a significant increase in apoptosis upon XBP1 gene silencing, with nearly a threefold increase in the number of apoptotic cells compared to normoxic conditions (Fig. 4j). This observation is consistent with the findings reported by another research group who investigated XBP1's role in tumor survival under hypoxia conditions [32].

5. Conclusion

To sum up, our study demonstrated the *in vitro* XBP1 gene silencing efficacy by using the targeted nanoparticles loaded with siRNA, thus promoting apoptosis in the challenging hypoxic conditions. These findings provide a strong foundation for advancing a safe and innovative TNBC treatment. Future investigations should prioritize *in vivo* studies to validate the efficacy and safety of this approach, bringing it one step closer to clinical applications.

CRediT authorship contribution statement

Meenu Mehta: Writing – review & editing, Writing – original draft, Validation, Methodology, Investigation, Formal analysis, Data curation, Conceptualization. **Thuy Anh Bui:** Writing – review & editing, Visualization, Investigation, Formal analysis, Data curation. **Andrew Care:** Writing – review & editing, Visualization, Supervision, Resources, Project administration. **Wei Deng:** Writing – review & editing, Visualization, Supervision, Resources, Project administration, Funding acquisition.

Declaration of competing interest

The authors declare that they have no known competing financial interests or personal relationships that could have appeared to influence the work reported in this paper.

Data availability

Data will be made available on request.

Acknowledgments

This work was financially supported by the funding (GNT1181889) from the Australian National Health and Medical Research Council, Deng's fellowship award (2019/CDF1013) from Cancer Institute NSW, Australia. Meenu Mehta is supported by the Research Training Program Scholarship (RTP). Andrew Care is supported by a Chancellor's Research Fellowship from the University of Technology Sydney (UTS).

References

[1] N.M. Almansour, Triple-negative breast cancer: a brief review about epidemiology, risk factors, signaling pathways, treatment and role of artificial intelligence, Front. Mol. Biosci. 9 (2022).
[2] M. Bou Zerdan, et al., Triple negative breast cancer: updates on classification and treatment in 2021, Cancers 14 (5) (2022).
[3] Y. Li, et al., Recent advances in therapeutic strategies for triple-negative breast cancer, J. Hematol. Oncol. 15 (1) (2022) 121.
[4] Q. Wu, et al., Multi-drug resistance in cancer chemotherapeutics: mechanisms and lab approaches, Cancer Lett. 347 (2) (2014) 159–166.
[5] J.J. Tao, K. Visvanathan, A.C. Wolff, Long term side effects of adjuvant chemotherapy in patients with early breast cancer, Breast 24 (0 2) (2015) S149–S153. Suppl 2.
[6] Y.J. Cheng, et al., Long-Term cardiovascular risk after radiotherapy in women with breast cancer, J. Am. Heart Assoc. 6 (5) (2017).
[7] S. Chen, et al., The emerging role of XBP1 in cancer, Biomed. Pharmacother. 127 (2020) 110069.
[8] Y. He, et al., Emerging roles for XBP1, a sUPeR transcription factor, Gene Expr. 15 (1) (2010) 13–25.
[9] W. Shi, et al., Unravel the molecular mechanism of XBP1 in regulating the biology of cancer cells, J. Cancer 10 (9) (2019) 2035–2046.
[10] X. Chen, et al., XBP1 promotes triple-negative breast cancer by controlling the HIF1α pathway, Nature 508 (7494) (2014) 103–107.
[11] N. Srivastava, et al., Hypoxia: syndicating triple negative breast cancer against various therapeutic regimens, Front. Oncol. 13 (2023) 1199105.
[12] L. Romero-Ramirez, et al., XBP1 is essential for survival under hypoxic conditions and is required for tumor growth, Cancer Res. 64 (17) (2004) 5943–5947.
[13] N. McCarthy, Hypoxia and XBP1S, Nat. Rev. Cancer 14 (5) (2014) 295, 295.
[14] N.B. Charbe, et al., Small interfering RNA for cancer treatment: overcoming hurdles in delivery, Acta Pharm. Sin. B 10 (11) (2020) 2075–2109.
[15] W. Ngamcherdtrakul, W. Yantasee, siRNA therapeutics for breast cancer: recent efforts in targeting metastasis, drug resistance, and immune evasion, Transl. Res. 214 (2019) 105–120.
[16] Y. Yao, et al., Nanoparticle-based drug delivery in cancer therapy and its role in overcoming drug resistance, Front. Mol. Biosci. 7 (2020) 193.
[17] L. Wang, B. Griffel, X. Xu, Synthesis of PLGA-lipid hybrid nanoparticles for siRNA delivery using the emulsion method PLGA-PEG-lipid nanoparticles for siRNA delivery, Methods Mol. Biol. 1632 (2017) 231–240.
[18] D.K. Jensen, et al., Design of an inhalable dry powder formulation of DOTAP-modified PLGA nanoparticles loaded with siRNA, J. Contr. Release 157 (1) (2012) 141–148.
[19] D. Sivadasan, et al., Polymeric lipid hybrid nanoparticles (PLNs) as emerging drug delivery platform-A comprehensive review of their properties, preparation methods, and therapeutic applications, Pharmaceutics 13 (8) (2021).
[20] T.O. Nielsen, et al., Immunohistochemical and clinical characterization of the basal-like subtype of invasive breast carcinoma, Clin. Cancer Res. 10 (16) (2004) 5367–5374.
[21] J.H. Mortensen, et al., Targeted antiepidermal growth factor receptor (cetuximab) immunoliposomes enhance cellular uptake in vitro and exhibit increased accumulation in an intracranial model of glioblastoma multiforme, J Drug Deliv 2013 (2013) 209205.
[22] D.C. Rio, et al., Purification of RNA using TRIzol (TRI reagent), Cold Spring Harb. Protoc. 2010 (6) (2010) pdb prot5439.
[23] M. Danaei, et al., Impact of particle size and polydispersity index on the clinical applications of lipidic nanocarrier systems, Pharmaceutics 10 (2) (2018).
[24] F. Fang, et al., EGFR-targeted hybrid lipid nanoparticles for chemo-photothermal therapy against colorectal cancer cells, Chem. Phys. Lipids 251 (2023) 105280.
[25] H. Masuda, et al., Role of epidermal growth factor receptor in breast cancer, Breast Cancer Res. Treat. 136 (2) (2012) 331–345.
[26] S. Acharya, F. Dilnawaz, S.K. Sahoo, Targeted epidermal growth factor receptor nanoparticle bioconjugates for breast cancer therapy, Biomaterials 30 (29) (2009) 5737–5750.
[27] W.D. Foulkes, I.E. Smith, J.S. Reis-Filho, Triple-negative breast cancer, N. Engl. J. Med. 363 (20) (2010) 1938–1948.
[28] L. Yin, et al., Triple-negative breast cancer molecular subtyping and treatment progress, Breast Cancer Res. 22 (1) (2020) 61.

[29] J. Gao, et al., The promotion of siRNA delivery to breast cancer overexpressing epidermal growth factor receptor through anti-EGFR antibody conjugation by immunoliposomes, Biomaterials 32 (13) (2011) 3459–3470.
[30] L. Zhang, et al., Systemic delivery of aptamer-conjugated XBP1 siRNA nanoparticles for efficient suppression of HER2+ breast cancer, ACS Appl. Mater. Interfaces 12 (29) (2020) 32360–32371.
[31] L. Zhang, et al., Development of targeted therapy therapeutics to sensitize triple-negative breast cancer chemosensitivity utilizing bacteriophage phi29 derived packaging RNA, J. Nanobiotechnol. 19 (1) (2021) 13.
[32] L. Romero-Ramirez, et al., XBP1 is essential for survival under hypoxic conditions and is required for tumor growth, Cancer Res. 64 (17) (2004) 5943–5947.